PHYSICAL REVIEW A VOLUME 16, NUMBER 3 SEPTEMBER 1977

# Field ionization of highly excited states of sodium*

T. F. Gallagher, L. M. Humphrey, W. E. Cooke, R. M. Hill, and S. A. Edelstein
*Molecular Physics Center, Stanford Research Institute, Menlo Park, California 94025*
(Received 11 March 1977)

We have observed the selective ionization of the degenerate $|m_j|$ levels of $s$, $p$, and $d$ states of sodium in the range of $n$ from 15 to 20 and have shown that atoms produced in these low-field ($\sim$ 10 V/cm) states pass adiabatically from low-field $|m_j|$ to intermediate-field $|m_l|$ states. Experiments on the Stark manifold states in intermediate fields ($\sim$ 1 kV/cm) and high fields ($\sim$ 4 kV/cm) show that the $|m_l| = 0$ and 1 states pass adiabatically from intermediate- to high-field states and that the passage of the $|m_l| = 2$ states is very nearly adiabatic. These findings suggest a general approach for predicting the threshold fields for ionization of atomic Rydberg states.

## I. INTRODUCTION

The field ionization of the lower excited states of hydrogen was investigated both experimentally and theoretically soon after the development of quantum mechanics.[1] After that advances in the field did not occur until relatively recently. Extensive numerical calculations of electric field ionization rates for hydrogen were performed by Rice and Good,[2] and also by Bailey *et al.*,[3] who extended the calculations up to $n = 20$. Recently Herrick[4] has calculated ionization rates for hydrogen using a variational approach. In recent experiments with fast hydrogen beams, Il'in[5] has resolved the ionization of the $n$ states in hydrogen from $n = 9$–$23$. Bayfield and Koch[6] have extended these measurements up to $n = 60$ by observing ionization of the $n = 63$–$69$ states of hydrogen. Both experiments are in agreement with the work of Bailey *et al.*

The development of the tunable dye laser has made it possible to populate single highly excited $n,l$ states efficiently. The ease and selectivity of the laser-excitation experiments has generated a renewed interest in the field ionization of high-lying or Rydberg states. Field ionization of highly excited states of Na, Xe, Cs, and Rb using laser excitation techniques has recently been reported.[7-10] In each of these investigations sharp thresholds were observed for field ionization and the threshold field was found to vary as $1/n^4$. Recently Littman *et al.*[11] have made direct measurements of the ionization rates for Na and have shown that the field ionization rates increase exponentially with the applied field as predicted by theory. However, the theoretical prediction that the higher-lying states of a Stark manifold should require higher fields for ionization is not borne out by their work. This discrepancy is attributed to the fact that the hydrogenic calculations assume no coupling of the Stark manifolds of different principal quantum number, which is not the case for sodium.

We have recently reported the resolution of the degenerate $|m_j|$ states in the field ionization of Na $d$ states[12] (we follow the usual convention that $L$, $S$, and $J$ are the electron's orbital, spin, and total angular momenta, respectively, and $m_l$, $m_s$, and $m_j$ are their projections in the field direction). Here we present a more detailed and extensive report of these investigations. In addition we present our further experimental observations and the conclusions drawn from them, which should be useful to anyone wishing to use field ionization as a selective Rydberg-state detector. The paper is logically divided into two parts. In the first we describe observations of the ionization of $s$, $p$, and $d$ states excited in low electric fields, the results of which show that atoms pass from the low-field states, where the total angular momentum $\vec{J}$ is a good quantum number, to the intermediate-field regime, where $\vec{L}$ and $\vec{S}$ are uncoupled, adiabatically when the field slew rate is $2 \times 10^{10}$ V/cm sec. In the second part of this paper, we describe experiments with the states of the $n = 17$ Stark manifold which give us an operational understanding of the passage from intermediate field to the high ionizing field. The question of how atoms pass through this field regime, where adjacent Stark manifolds overlap, is obviously complicated because there are several level crossings between zero field and the high electric field required for ionization. In these experiments we have taken the pragmatic approach of determining whether the passage from intermediate to high field, through these crossings, is adiabatic or diabatic with a slew rate of $2 \times 10^{10}$ V/cm sec. Under these conditions we find that the passage is almost always adiabatic, implying that the passage will also be adiabatic for lesser slew rates. Although there are minor ambiguities in this approach, these studies illuminate many of the general features of field ionization of sodium Rydberg states and, taken together, enable

us to draw general conclusions about the field ionization process which should be applicable to other atoms. It is our hope that the practical insights presented here will be useful in planning experiments using field ionization as a selective Rydberg atom detector.

## II. EXPERIMENTAL METHOD AND APPARATUS

The general approach is shown in Fig. 1. An atomic sodium beam passes between a plate and a grid where it is crossed by two laser beams which pump the sodium atoms in two steps from the $3s$ to $3p$ state and from the $3p$ state to a high $s$ or $d$ state (or the $s$ or $d$ component of a Stark mixed state). By choosing which of the $3p_{1/2}$ or $3p_{3/2}$ states we use as the intermediate state, we can take advantage of the $\Delta J$ selection rules to selectively populate the fine-structure levels of highly excited $p$ and $d$ states.[13] About 1 $\mu$sec after the laser pulse, a high-voltage pulse is applied to the lower plate, field ionizing the Rydberg atoms and accelerating the ions formed into the electron multiplier. The ion signal from the multiplier is then amplified and put into an oscilloscope or a boxcar averager, the output of which is recorded on an $x$-$y$ recorder. Figure 2 is a timing diagram showing the relevant events of the experiment. Note that the ion pulse is detected at or before the peak of the ionization pulse so that the details of the shape of the ionizing pulse after its peak are unimportant.

The beam apparatus is contained entirely in a 45-cm diameter vacuum chamber which is pumped by an NRC-Varian VHS-6 pump. Typical operating pressures are $10^{-7}$–$10^{-6}$ Torr. We have raised the pressure to $>10^{-5}$ Torr without a noticeable signal due to collisional ionization. The atomic beam source is a stainless-steel tube 0.95 cm in diameter by 15-cm long which has a 0.5-mm diameter hole halfway down its length through which the atomic beam effuses. The oven is half-filled with sodium, its ends crimped, and then clamped to high current feedthroughs on the source flange. The oven is heated by passing 25 A of ac current through it. The oven is 10 cm from the interaction region and produces a beam with a density of $10^{8}$–$10^{10}$ atoms/cm$^3$ in the interaction region.

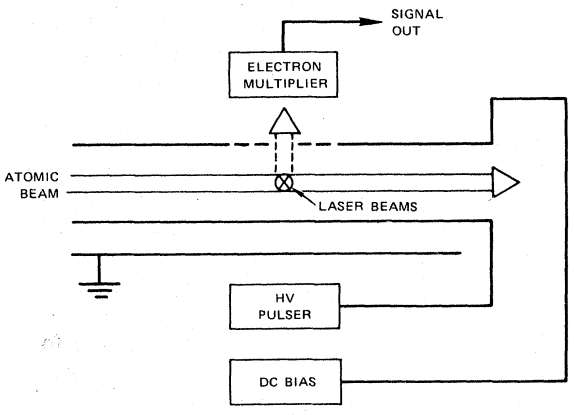


FIG. 1. Essence of the apparatus. The atomic beam passes between a plate and a grid where it is crossed by the laser beams. After the laser pulses, a high-voltage pulse is applied to the plate, ionizing the Rydberg atoms and accelerating the ions to the electron multiplier.

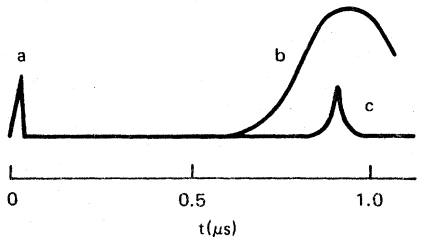


FIG. 2. Timing diagram for the experiment. The fast (4 nsec) laser pulses (a) are at $t=0$, and the ionizing pulse (b) is applied 0.5 $\mu$sec later. During the high-voltage pulse, the 50-nsec wide ion signal (c) is detected.

The high-voltage pulser is built using a commercial trigger transformer for a flashlamp. It is triggered by a pulse of ~3 V and can produce pulses of up to 10 kV. As indicated by Fig. 2 the ionizing pulse increases to a peak voltage then decreases. The pulse voltage has a risetime of 0.3 $\mu$sec and is within 5% of the peak voltage for 0.2 $\mu$sec before decaying. Thus what we observe as a threshold field for ionization is one high enough to produce an electric field ionization rate of $10^{7}$ sec$^{-1}$.

As shown schematically in Fig. 1, the ionizer assembly is a plate and a grid both $7.5 \times 10$ cm (the grid itself is $2.5 \times 5$ cm in the center of the upper plate). The grid is made of 0.5-mm mesh nickel wire. The plate-to-grid spacing is 1.110 or 1.124 cm depending on whether metal or insulating spacers are used to mount the grid plate. This geometry is adequate to resolve the $|m_l|$ thresholds, but we found that when the plate-to-grid spacing was reduced to 0.5 cm the $|m_l|$ thresholds overlapped, presumably due to the greater field inhomogeneities produced by moving the grid closer to the plate.

The electron multiplier is an EMI venetian blind multiplier which is wired with capacitors on the last dynodes in the same way a photomultiplier tube is wired for pulsed operation. This is necessary because the multiplier output currents are ~1 mA. The intensity of the atomic beam is measured with a tungsten hot-wire detector. To tune the

resonance line laser we observe the resonance fluorescence from the atomic beam using a light pipe to the exterior and a 1P28 photomultiplier tube. The lasers used for these experiments are nitrogen-laser pumped dye lasers. The nitrogen laser is of a transmission line design and has the following characteristics: 2 mJ pulse energy, 4 nsec full width at half maximum (FWHM) pulse-width, and 20 Hz repetition rate. The dye lasers are of the Hänsch design,[14] using a transversely pumped dye cell, grating, beam expanding telescope, and 20% reflecting front mirror. The dye lasers have 50-$\mu$J pulses in a 0.15-Å (FHWM) bandwidth. A small synchronous motor attached to the rotation stage of the grating of the laser used to pump the $3p \rightarrow ns$ or $nd$ transition allows us to scan the wavelength of that laser.

### III. $s$, $p$, AND $d$ STATE EXPERIMENTS

In our studies of the $s$, $p$, and $d$ state ionization thresholds we found that for each state the number of ionization thresholds is equal to the number of $|m_j|$ states. Consequently, the appearances of the ionization thresholds for $s$, $p$, and $d$ states are quite different. Examples of ionization thresholds are shown in Figs. 3, 4(a), and 5(a), which are scans of ionization current versus peak ionizing field for the 18$s$, 17$p$, and 17$d$ states, respectively. In Fig. 4(a) there are two thresholds for the $17p_{3/2}$ state at 4.44 and 4.70 kV/cm. The $17p_{1/2}$ state has only one threshold at 4.70 kV/cm (there is a vestigial threshold at 4.44 kV/cm which we attribute to the state mixing effects of the electric field). In Fig. 5 there are three thresholds for the $17d_{5/2}$ state at 4.36, 4.63, and 5.17 kV/cm. Note that in all cases the number of thresholds observed equals the number of $|m_j|$ states.

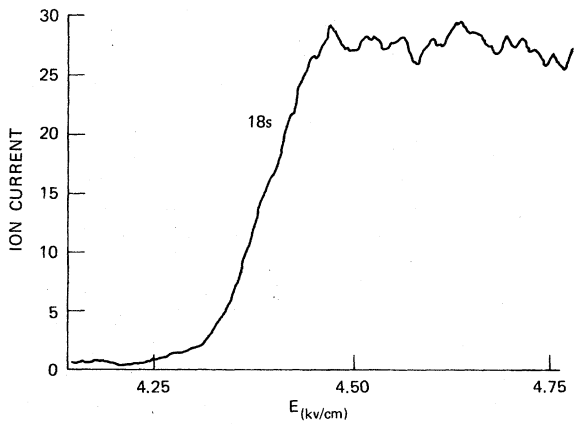


FIG. 3. 18$s$ ionization threshold. The field ionization current is plotted vs the peak ionizing field.

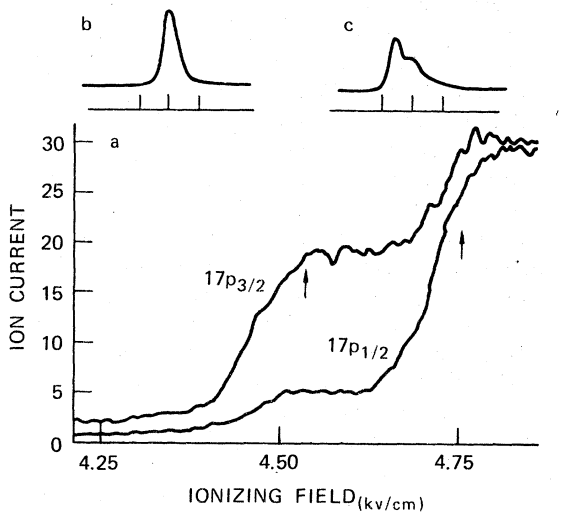


FIG. 4. (a) $17p_{1/2}$ and $17p_{3/2}$ ionization thresholds. The field ionization current is plotted vs the peak ionizing field. (b) The time-resolved signal when the peak ionizing field is 4.51 kV/cm. The horizontal time scale is 50 nsec/division. (c) The time-resolved signal when the peak ionizing field is 4.76 kV/cm. The horizontal time scale is 50 nsec/division. Note that there are two peaks and the first one has moved to an earlier time. In both (b) and (c) the center time mark corresponds to the peak of the ionizing pulse.

In the ionization of a state which has more than one threshold, such as the $p_{3/2}$ state, the threshold can be time resolved. This is true because the ionizing field increases in time and reaches each of the ionization thresholds at different times

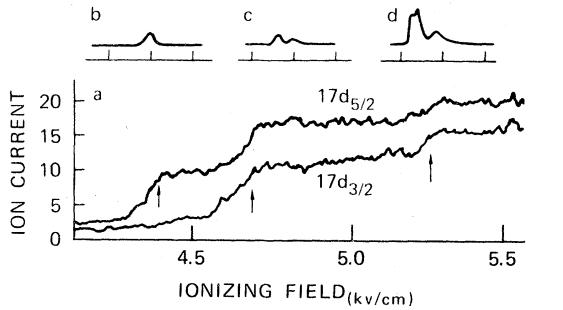


FIG. 5. (a) Experimental traces of the ion current vs peak ionization voltage for the $17d_{3/2}$ and $17d_{5/2}$ states. The approximate locations of the $|m_l|=0,1$, and 2 thresholds are indicated by arrows. (b), (c), (d) Oscilloscope traces of ion signals at different peak ionizing fields. In each case the center time marker corresponds to the peak of the ionizing high-voltage pulse. The horizontal scale is 200 nsec/division. (b) $|m_l|=0$ ion pulse, peak field = 4.58 kV/cm. (c) $|m_l|=0$ followed by $|m_l|=1$ ion pulse, peak field = 4.98 kV/cm. (d) $|m_l|=0$ overlapping $|m_l|=1$ followed by $|m_l|=2$ ion pulse, peak field = 5.27 kV/cm.

with the result that the ion signals can be time resolved. Figures 4(b) and 4(c) show the oscilloscope traces of time-resolved ion signals from the $17p_{3/2}$ state at 4.51 and 4.76 kV/cm peak ionizing fields. In Fig. 4(b) there is a single ion pulse. In Fig. 4(c) there are two barely resolved pulses, one corresponding to each ionization threshold. Note that the first ion pulse is earlier in Fig. 4(c) than in Fig. 4(b) because the ionizing field reaches the first threshold sooner. Analogous time-resolved ion signals can be seen in the ionization of the $17d_{5/2}$ state. In Figs. 5(b), 5(c), and 5(d) we show oscilloscope traces of the $17d_{5/2}$ ion signals at peak ionizing fields of 4.58, 4.98, and 5.27 kV/cm. Note that in Figs. 5(c) and 5(d) the first ion peak appears at an earlier time than in Fig. 5(b) since the ionizing field reaches the first ionization threshold sooner. Although the first and second peaks are well resolved in Fig. 5(c) they are barely resolved in Fig. 5(d). This occurs because as the peak voltage is increased, they are ionizing at a point earlier in the pulse where the field is increasing faster in time resulting in a shorter time for the field to increase from the first threshold to the second. In practice the time resolution of the ion peaks is very useful in distinguishing between the states.

To assign low- and high-field quantum numbers to the observed thresholds, we must first consider the sequence of events in the experiment. The atoms are excited in a very low field where the fine structure $|m_j|$ states are the good quantum states, then the electric field is increased to a very high value to ionize the atoms. In the high ionizing field the $|m_l|$ states are the good quantum states. So it is the final $|m_l|$ state of the atom which determines the ionization threshold. To make the assignments we must consider to what extent the passage from low to high field is adiabatic or diabatic. If the field were increased at an infinitesimal rate from low to high field, there would be a gradual adiabatic evolution from one initial low-field state to one high-field state. If on the other hand, the field changed instantaneously from low to high field, the passage would be diabatic and the initial low-field state would in most cases be projected onto several high-field states.

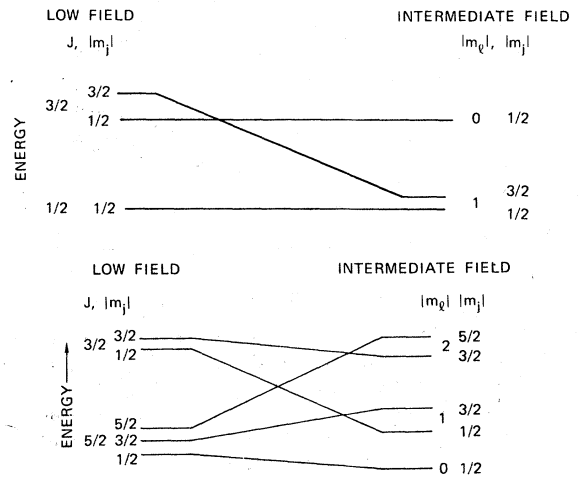


FIG. 6. (a) Adiabatic correlation diagram for the $p$ states obtained from the known $p$ state fine-structure splitting and applying the no-crossing rule. (b) Adiabatic correlation diagram for the $d$ states obtained in the same way.

It is convenient to define three field-strength regimes: low field, where the fine-structure interactions are stronger than the Stark effect; intermediate field, where the Stark effect is stronger than the fine-structure interactions but less than the term separation (in this regime the Stark manifolds from adjacent $n$ states do not overlap); and high field, where the Stark energy is greater than the term separation and the Stark manifolds from adjacent $n$ states overlap. Since $|m_l|$ is a good quantum number in both intermediate- and high-field regimes, the passage from $|m_j|$ to $|m_l|$ states occurs between low and intermediate field. Thus for the purpose of assigning quantum numbers to the thresholds, we need only understand the passage from low to intermediate field.

Let us first consider the effect of a diabatic passage. A diabatic passage would simply project both the $17p_{1/2}$ and $17p_{3/2}$ fine-structure states onto the $|m_l| = 0$ and 1 states with the result that we would see two ionization thresholds for each fine-structure state. However, as shown in Fig. 4(a), the $17p_{1/2}$ state has only one threshold and the $17p_{3/2}$ state has two. Consequently, we must conclude that the passage is adiabatic, that is, each of the $17p$ $|m_j|$ states evolves gradually into the corresponding intermediate-field $|m_l|$ state. Similarly, both the $17d_{3/2}$ and $17d_{5/2}$ fine-structure states would have three ionization thresholds if the passage were diabatic, but as shown in Fig. 5(a) there are only two thresholds for the $17d_{3/2}$ state so that the low- to intermediate-field passage is adiabatic. Since the low to intermediate field passage is adiabatic, we may correlate the states in these two field regimes by applying the no-crossing rule, that is, states of the same total $m$, $m_j$ do not cross in passing from low to intermediate field.[15] It is worth noting that while $J$ is not a good quantum number in the intermediate-field region, $m_j = m_l + m_s$ is still meaningful. In Fig. 6 we show the correlation diagrams for the $p$ and $d$ states. The correla-

tion diagram for the $p$ state is constructed by imposing two constraints. First, the $p$ fine structure is normal, so the $J=\frac{3}{2}$ state lies above the $J=\frac{1}{2}$ state in low field, and second the $J=\frac{3}{2}$ state has two thresholds and must therefore connect to two intermediate-field $|m_l|$ states. The correlation diagram of Fig. 6(a) is the only ordering of intermediate-field states which satisfies both requirements. This alone is enough information to assign the first threshold (at 4.44 kV/cm) of Fig. 4(a) as $|m_l|=0$ and the second (at 4.70 kV/cm) as $|m_l|=1$. From Fig. 6(a) we can determine the low-field assignments of the thresholds as well. Both high- and low-field assignments are given in Table I.

In a similar manner the correlation diagram of the $d$ state shown in Fig. 6(b) can be constructed. The $d$-state fine structure is inverted so the $J=\frac{3}{2}$ state lies above the $J=\frac{5}{2}$ state in low field. The observation of two thresholds for the $J=\frac{3}{2}$ and three for the $J=\frac{5}{2}$ states implies that they correlate with two and three $|m_l|$ states, respectively. The only correlation diagram which satisfies both requirements is shown in Fig. 6(b). From Fig. 6(b) alone we are able to assign the first threshold at 4.36 kV/cm which comes only from the $d_{5/2}$ state as $|m_l|=0$. To distinguish between the $|m_l|=1$ and 2 states we took advantage of the $\Delta m$ selection rules. We applied a low (~2 V/cm) dc field and polarized the $3p_{3/2}$-$17d_{5/2}$ laser parallel and perpendicular to the dc field. With $\vec{E}_{\text{laser}} \parallel \vec{E}_{\text{dc}}$ only $\Delta m=0$ transitions are allowed and it is not possible to populate $|m_j|=\frac{5}{2}$ states. With $\vec{E}_{\text{laser}} \perp \vec{E}_{\text{dc}}$ all the $m_j$ states can be populated since both $|m_j|=\frac{1}{2}$ and $\frac{3}{2}$ are populated in the $3p_{3/2}$ state. With $\vec{E}_{\text{laser}} \parallel \vec{E}_{\text{dc}}$ the third threshold (at 5.17 kV/cm) of the $d_{5/2}$ state completely disappeared, identifying it as the $|m_j|=\frac{5}{2}$, $|m_l|=2$ threshold. Thus, by elimination, the second threshold (at 4.63 kV/cm) corresponds to the $|m_l|=1$ state. From Fig. 6(b), it is straightforward to assign the low-field quantum numbers. In Table I, both the low- and high-field assignments of the thresholds are given. The assignment of an $s$ state is trivial since it can only be $|m_j|=\frac{1}{2}$ in low field and $|m_l|=0$ in high field.

TABLE I. Threshold fields and low and intermediate field state assignments for the $18s$, $17p$, and $17d$ states.

| State | Low field assignment $J, \lvert m_j\rvert$ | Intermediate field assignment $\lvert m_l\rvert$ | Threshold field (kV/cm) |
|---|---|---|---|
| $18s$ | $\frac{1}{2},\frac{1}{2}$ | 0 | 4.40 |
| $17p$ | $\frac{1}{2},\frac{1}{2}$ | 1 | 4.70 |
| | $\frac{3}{2},\frac{1}{2}$ | 0 | 4.44 |
| | $\frac{3}{2},\frac{3}{2}$ | 1 | 4.70 |
| $17d$ | $\frac{3}{2},\frac{1}{2}$ | 1 | 4.63 |
| | $\frac{3}{2},\frac{3}{2}$ | 2 | 5.17 |
| | $\frac{5}{2},\frac{1}{2}$ | 0 | 4.36 |
| | $\frac{5}{2},\frac{3}{2}$ | 1 | 4.63 |
| | $\frac{5}{2},\frac{5}{2}$ | 2 | 5.17 |

TABLE II. Threshold fields required to produce an ionization rate of $10^7$ sec$^{-1}$ in $s$, $p$, and $d$ states of Na. The values are ±4% and are given in kV/cm.

| State | $\lvert m_l\rvert=0$ | $\lvert m_l\rvert=1$ | $\lvert m_l\rvert=2$ | $\lvert m_l\rvert=2$ | $\lvert m_l\rvert=2$ |
|---|---|---|---|---|---|
| $16s$ | 7.36 | | | | |
| $17s$ | 5.77 | | | | |
| $18s$ | 4.40 | | | | |
| $19s$ | 3.62 | | | | |
| $20s$ | 2.80 | | | | |
| $21s$ | 2.32 | | | | |
| $16p$ | 5.83 | 6.06 | | | |
| $17p$ | 4.44 | 4.70 | | | |
| $18p$ | 3.46 | 3.65 | | | |
| $19p$ | 2.79 | 2.88 | | | |
| $15d$ | 7.42 | 7.74 | 8.62 | | |
| $16d$ | 5.48 | 6.05 | 6.43 | | |
| $17d$ | 4.36 | 4.63 | 5.17 | | |
| $18d$ | 3.40 | 3.53 | 3.88 | 4.11 | 4.32 |
| $19d$ | 2.74 | 2.81 | 3.03 | 3.28 | 3.54 |
| $20d$ | 2.22 | 2.30 | 2.48 | 2.62 | 2.73 |

We have measured the thresholds for a series of $s$, $p$, and $d$ states with the results given in Table II. As shown by Table II the ordering of the thresholds for all the $p$ and $d$ states is the same as the examples of the $17p$ and $17d$ states so the low-field assignments of all these states may be made in an analogous fashion.

## IV. STARK MANIFOLD STATE EXPERIMENTS

The experiments described in the previous section show that atoms pass adiabatically from low-field $|m_j|$ states to intermediate-field $|m_l|$ states. However, these experiments do not give us much insight into how the atoms pass from intermediate to high field. Because the $|m_l|=0$ and 1 states always show only one threshold, we at least know that they pass from intermediate to high field by a unique path, which we previously[13] suggested was probably adiabatic. On the other hand, as shown by Table II, the $|m_l|=2$ states show multiple thresholds in some cases so that the intermediate-to-high-field pas-

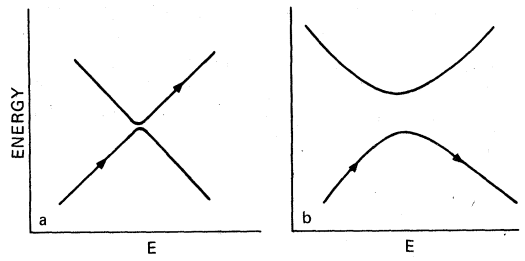


FIG. 7. (a) Plot of the energies of two states as a function of electric field $E$ for the case of weak coupling between the states. The energy gap between the two curves is small and as the ionizing field is applied, the atom traverses the crossing diabatically as shown by the arrow, crossing the energy gap. (b) The same for the case of stronger coupling. As the ionizing field is applied, the atom traverses the avoided crossing adiabatically with no level crossing as shown by the arrows.

sage is clearly neither wholly adiabatic nor wholly diabatic. In order to clarify the nature of the intermediate-to-high-field passage we have done the experiments in intermediate and high fields which are described in this section.

For $n \sim 17$ at fields >1 kV/cm adjacent Stark manifolds overlap, and if we neglect any coupling between the manifolds, many states of the same $|m_l|$ cross. However, the coupling is nonzero, and in reality the levels do not cross but have avoided crossings. If the coupling is weak, the energy gaps of the avoided crossings are small as shown by Fig. 7(a), a plot of the energy levels at an avoided crossing. If the coupling is stronger, the avoided crossing has a larger energy gap as shown as Fig. 7(b). Let us assume that when the ionizing field is applied, the atom passes through the avoided crossing of Fig. 7(a) in a time short compared to the inverse of its energy gap. In this case the atom will traverse the avoided crossing diabatically, crossing the energy gap as shown by the arrows of Fig. 7(a). On the other hand, let us assume that the passage of the atoms through the crossing of Fig. 7(b) requires a time long compared to the inverse of the energy gap, in which case the avoided crossing will be traversed as shown by the arrows of Fig. 7(b). Note that in Fig. 7(b) the noncrossing rule is followed, but in Fig. 7(a) it is not. Obviously if the crossing is traversed in a time comparable to the inverse of the energy gap the passage will neither be wholly diabatic nor wholly adiabatic, resulting in multiple paths and thus multiple ionization thresholds. Most of the states observed have single thresholds, so that we have concluded that most of the crossings are traversed either wholly adiabatically or diabatically.

An atom traverses several level crossings in passing from intermediate to high field, and although in principle it would be desirable to examine each level crossing in detail from a practical point of view, it is only the overall effect of traversing all the crossings which is important. In the experiments described in this section we have addressed the practical question to what extent is the intermediate-to-high-field passage adiabatic or diabatic with respect to $|m_l|$ when the slew rate of the electric field is $\sim 2 \times 10^{10}$ kV/cm sec. The easiest way to see how one might go about this is to consider as a hypothetical example the extreme $m_l = 0$ components of the $n = 17$ Stark manifold. It is a straightforward matter to make good estimates of the adiabatic and diabatic paths from intermediate to high field for these states.

The diabatic paths can be estimated by assuming that the interactions with the Stark levels of other $n$ manifolds are negligible so that all level crossings are traversed diabatically, i.e., the atom crosses levels. Thus, the diabatic paths are simply given by the hydrogenic energy dependence of the states on electric field, ignoring interactions with other $n$ manifolds. The diabatic paths are shown by the broken lines of Fig. 8. The adiabatic paths reflect the opposite extreme, the situation in which the $n$ manifolds are well coupled so that all the avoided crossings are traversed adiabatically, i.e., the noncrossing rule applies. In this case the path will follow the hydrogenic energy level out to the field at which the Stark states from adjacent manifolds intersect, where states of the same $m_l$ will mutually repel. As a result, the energy of the adiabatic path remains essentially constant as the atom goes to higher fields, as shown by the solid lines of Fig. 8. In a similar manner the diabatic paths of the extreme components of the $n = 16$, 18, and 19 manifolds are shown in Fig. 8 at fields up to 3 kV/cm by broken lines. The adiabatic paths up to 3 kV/cm for these states are shown by solid lines. For simplicity we have omitted $s$ and $p$ states from this picture. The diabatic paths of the extreme components show when the Stark manifolds of adjacent $n$ states intersect, which as shown by Fig. 8 is at a field of ~1.5 kV/cm for $n = 17$.

As shown by Fig. 8 the two paths are quite different so that it should be possible to differentiate between them. To do this, we can do an experiment consisting of two parts. First, we selectively excite each of the two extreme states in an intermediate field of ~1 kV/cm (where the Stark states are separated by more than the laser linewidth) and measure their ionization thresholds. Let us say the two threshold fields are 5 and 4 kV/cm for the lower and upper extreme states, respec-

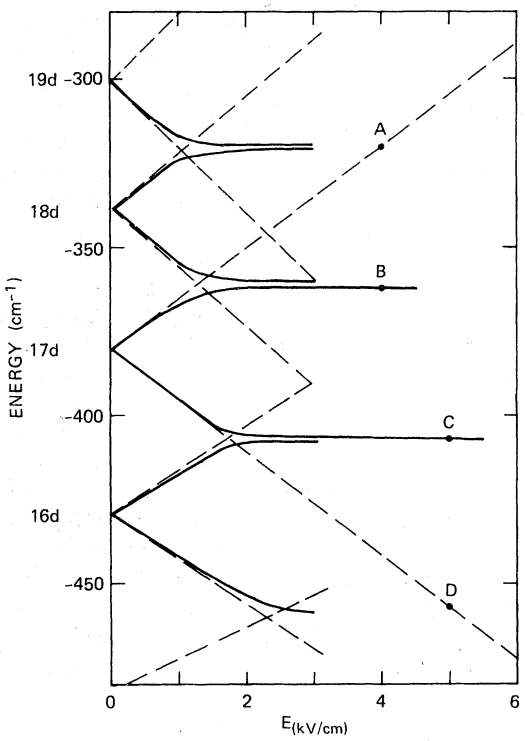


FIG. 8. A plot of the energy levels in an electric field showing the diabatic (---) and adiabatic (——) paths from low to high field for the two extreme components of the $n=17$ manifold. The labeled points indicate hypothetical measured energies and threshold fields for these states. If the states ionize at points A and D, the passage is diabatic; if the states ionize at points B and C, the passage is adiabatic.

tively. Now we know the field at which each initially excited state ionized with a rate of $10^7$ sec$^{-1}$. If we knew in addition the energy of each of these states when it ionized with a rate of $10^7$ sec$^{-1}$ we could tell if that state was close to the diabatic or adiabatic path when it ionized. For example, if the energy of the upper manifold state was $-320$ cm$^{-1}$ when it ionized, the state would have been at point A on Fig. 8 at ionization, a point which is clearly on the diabatic path. If, however, the energy of the state was found to be $-360$ cm$^{-1}$ at ionization, then the passage would go through point B, which is on the adiabatic path.

Similarly, if the lower manifold state was found to have an energy of $-410$ cm$^{-1}$ at ionization, the atom would be at point C ionization, a point on the adiabatic path. On the other hand, if its energy was found to be $-460$ cm$^{-1}$ at ionization, corresponding to point D, it would be on the adiabatic path. By the very nature of the adiabatic passage, the energy spread of the manifold at ionization is very nearly equal to the term separation at $n=17$, about 90 cm$^{-1}$, if the passage is adiabatic. If on the other hand, the passage is diabatic, the energy spread at ionization of the two extreme components will be ~300 cm$^{-1}$. Because of the substantial difference in the energies of the states at ionization, depending whether the path is adiabatic or diabatic, it should be quite easy to identify the ionization path using this method.

Although it should be possible to do this experiment using only the two extreme components of the manifold, as the preceding example shows, for completeness we have studied all the $|m_l|=0$, 1, and 2 states of the $n=17$ manifold. As in the previous illustration there are two parts to the experiment. First, we excite the $n=17$ Stark manifold states in an intermediate field (~1 kV/cm) and measure their ionization thresholds for an ionization rate of $10^7$ sec$^{-1}$. In the second part of the experiment, at high fields (~4 kV/cm), we determine the energies and fields at which states ionize with a rate of $10^7$ sec$^{-1}$. Since we know the threshold field $E_t$ for a state initially excited in intermediate field from the first part of the experiment, we can determine its energy at ionization from the second part by finding the energy at which a state requires a field $E_t$ to ionize with a rate of $10^7$ sec$^{-1}$.

To identify and measure the ionization thresholds of the $n=17$ manifold, we excited the atoms in a dc field of 893 V/cm and scanned the second laser with $\vec{E}_{laser} \| \vec{E}_{dc}$ (to excite $|m_l|=0$ and 1) and with $\vec{E}_{laser} \perp \vec{E}_{dc}$ (to excite $|m_l|=0$, 1, and 2) to locate the states. At this field the Stark components are ~0.4 Å apart and are easily resolved with the laser. For convenience we have labeled the states from 1 to 16 in order of increasing energy (decreasing binding energy) as shown in Fig. 9. State

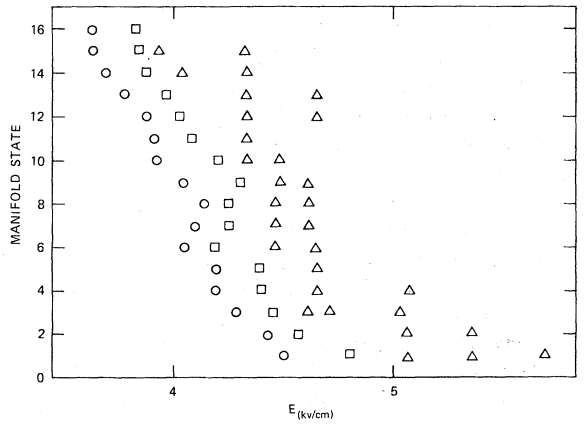


FIG. 9. Ionization threshold fields for the $|m_l|=0$ (○), $|m_l|=1$ (□), and $|m_l|+2$ (△) $n=17$ Stark manifold states. Note in particular that several of the $|m_l|=2$ states show the same thresholds.

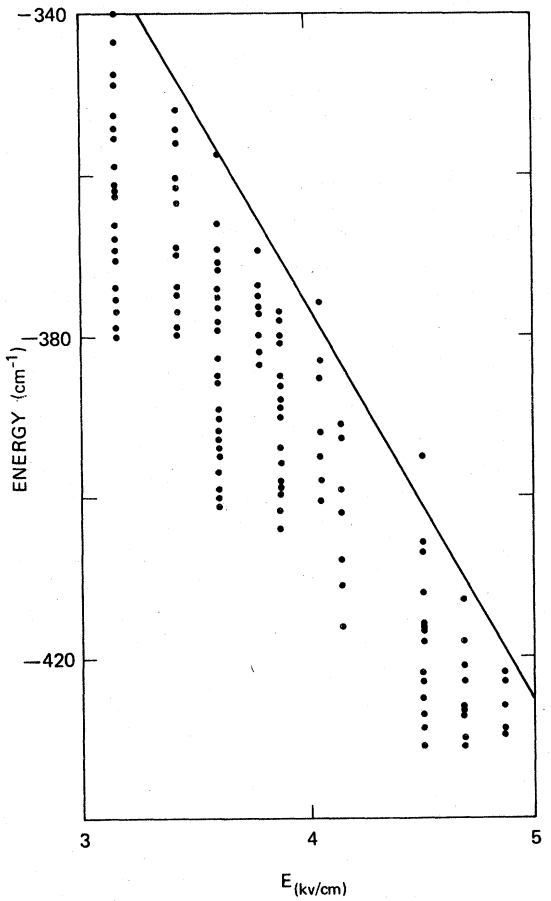


FIG. 10. A plot of laser scans in high dc fields showing the locations of $|m_l|=0$ and 1 states with field ionization rates less than $10^6$ sec$^{-1}$. Note that in general higher-lying states ionize at lower fields. The line indicates the boundary for an ionization rate of $10^6$ sec$^{-1}$ for $|m_l|=1$ states.

1 corresponds to the 17$d$ state in low field, and state 16 corresponds to the 18$p$ state in low field. The threshold fields for ionization were measured with the results shown in Fig. 9. Note that in many cases several $|m_l|=2$ states show the same threshold indicating that they are ionizing via the same final state. As shown by Fig. 9, higher-energy states generally have lower ionization thresholds. In the low-field studies of $p$ and $d$ states, we observed that $|m_l|=0$ states always have lower ionization thresholds than $|m_l|=1$ states. Since the two extreme components of the manifold are the adiabatic continuations fo the 17$d$ and 18$p$ states, we know that the first threshold observed is $|m_l|=0$ and the second $|m_l|=1$. We have assumed that this ordering holds for the entire $n=17$ manifold. The $|m_l|=2$ states can be unambiguously assigned using the polarization of the laser.

The second part of the manifold study is the excitation of the atoms in high fields to measure the energy of the states when they have ionization rates = $10^6$ sec.$^{-1}$ We have done this using the method of Littman *et al.*[11] The atoms are excited in a high dc field (~4 kV/cm) and an ionizing pulse of ~2 kV/cm is applied 2 $\mu$sec later. The boxcar gate is delayed to accept only the ions produced by the ionizing pulse. Consequently, atoms which are excited but field ionize at a rate $\geq 10^6$ sec$^{-1}$ are not observed by the boxcar averager. By taking laser scans at various dc fields we can see where the levels disappear as a result of ionization (at a rate of $10^6$ sec$^{-1}$). Figures 10 and 11 show the results of the high-field scans. The dots in Fig. 10 indicate the positions of observed $|m_l|=0$ and 1 levels which have field ionization rates $<10^6$ sec$^{-1}$. In the region with no dots all states have ionization rates $>10^6$ sec$^{-1}$. Figure 11 is the same for the $|m_l|=2$ states. In both Figs. 10 and 11 the lines indicate a linear approximation to a boundary for an ionization rate of $10^6$ sec$^{-1}$. Since the threshold field experiments described in the preceding section

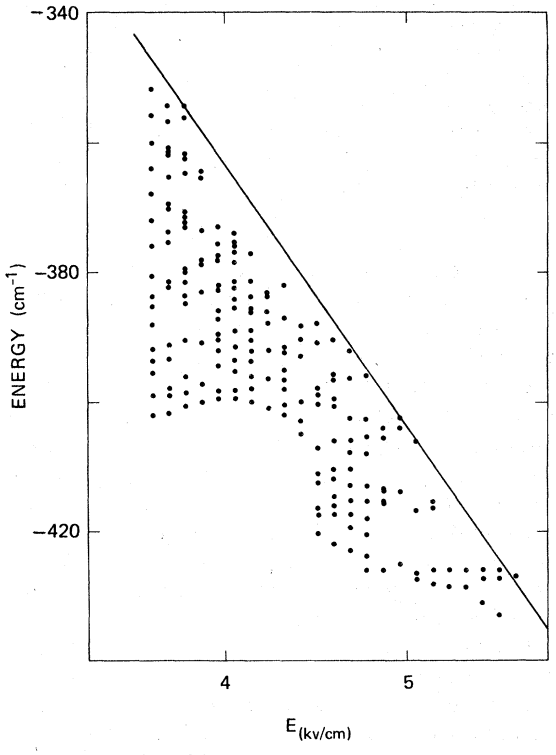


FIG. 11. A plot of laser scans in high dc fields showing the locations of $|m_l|=2$ states with field ionization rates less than $10^6$ sec$^{-1}$. As in Fig. 8 the higher-energy states ionize at lower fields. Also, the $|m_l|=2$ states ionize at higher fields than the $|m_l|=0$ and 1 states. The line indicates the boundary for an ionization rate of $10^6$ sec$^{-1}$.

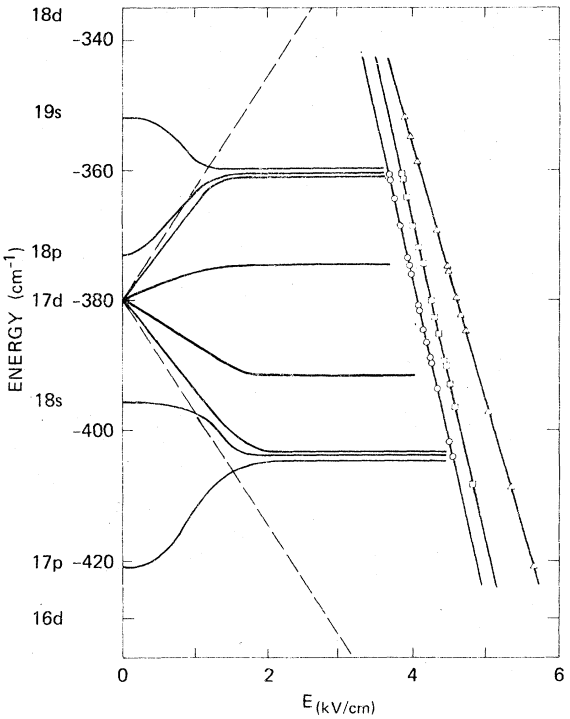


FIG. 12. A plot of the energy levels in an electric field near $n = 17$. The solid lines show the approximate adiabatic paths for the states from $17p$ to $19s$ including the two extreme components of the $n = 17$ manifold as well as two intermediate components. The broken lines indicate the diabatic paths for the extreme $n = 17$ Stark components. The $|m_l| = 0$ (○), $|m_l| = 1$ (□), and $|m_l| = 2$ (△) manifold state thresholds are plotted on the boundary lines for an ionization rate of $10^7$ sec$^{-1}$ for each of these states to show that they follow adiabatic paths from intermediate to high fields.

show that the $|m_l| = 0$ states ionize at ~4% lower fields than the $|m_l| = 1$ states, we attribute the boundary in Fig. 10 to the $|m_l| = 1$ states.

We are now able to use these data to construct a diagram similar to Fig. 8. In Fig. 12, we have drawn, with broken lines, the diabatic paths for the extreme components of the $n = 17$ manifold. The adiabatic paths of the extreme components and two of the intermediate components are shown by solid lines. In fact, there are three adiabatic paths between each of the adiabatic paths shown in Fig. 12. In reality these paths are not completely straight at fields >1 kV/cm, but for the purposes of this discussion that is not important. The adiabatic paths of the $17p$, $18p$, $18s$, and $19s$ levels (which are simply determined by application of the no-crossing rule) are also shown for completeness.

To compare the observed ionization thresholds of the intermediate-field states which are for an ionization rate of $10^7$ sec$^{-1}$ with the high-field data which are for an ionization rate of $10^6$ sec$^{-1}$ we must first adjust the high-field data to correspond to an ionization rate of $10^7$ sec$^{-1}$. This is a simple correction to make. From the results of Littman *et al.*[11] we conclude that a $3\frac{1}{2}\%$ increase in the ionization field raises the ionization rate from $10^6$ to $10^7$ sec$^{-1}$. Using this simple correction we can plot the $10^7$ sec$^{-1}$ ionization rate boundary lines for the $|m_l| = 1$ and 2 states on Fig. 12, using the $10^6$ sec$^{-1}$ ionization rate boundary lines of Figs. 10 and 11. The $|m_l| = 0$ boundary line of Fig. 12 is obtained by lowering the field of the $|m_l| = 1$ boundary by 4%.

Now we may plot the observed $|m_l| = 0$, 1, and 2 ionization thresholds on their respective boundary lines to determine the energies of each of these states when they are ionized. Essentially this procedure amounts to using the threshold ionization field as a parameter to link the initial state with its energy at ionization.

As shown by Fig. 12, the $|m_l| = 0$ and 1 states obviously fall within the adiabatic paths for the two exteme components. The $|m_l| = 2$ states go clearly outside the adiabatic paths but are not at all near the diabatic paths. Thus, we can definitely say that for slew rates $\leq 2 \times 10^{10}$ V/cm sec the $|m_l| = 0$ and 1 state passage is completely adiabatic and the $|m_l| = 2$ passage is very nearly adiabatic.

As shown by Fig. 9, some of the $|m_l| = 2$ states exhibit multiple thresholds which can result from partially diabatic traversals of bound-state level crossings resulting in several final ionizing states or peaks in the ionization rate of one state as observed by Littman *et al.*[11] which could lead to a single state having more than one ionization threshold (it is worth noting that the situation in which one state has more than one ionization threshold would be caused by partially diabatic traversals of level crossings with states which have ionization rates in excess of $10^7$ sec$^{-1}$). Although in our high-field scans, such as Figs. 10 and 11, we saw no level disappearance effects due to level crossings with unbound states such as those described in Ref. 11, we are not able to rule out the possibility that they are present. Consequently at this point the cause of the multiple thresholds is still an open question. In any event it is clear from Fig. 12 that this minor ambiquity does not materially affect our general conclusions.

## V. DISCUSSION

Our observation that the states of one manifold ionize in order of increasing binding energy, the opposite order from the theoretical prediction is

of course consistent with the observation of adiabatic passage from low to high field. The adiabatic passage demonstrates that there is coupling between the Stark manifolds of different $n$ states, supporting the previous suggestion that the discrepancies between the observed results in sodium and the theoretical calculations for hydrogen are due to coupling of overlapping Stark manifolds of different $n$ states.[11]

Our observations suggest a useful way of treating the observed ionization thresholds of the $s$, $p$, and $d$ states excited in low field. In previous work[7-10] it has been shown that the field required for ionization varies as $n^{-4}$, that is as the square of the binding energy $W$. Our observation that the field required to ionize an atom increases with its binding energy in the high ionizing field suggests that we try to fit the ionization thresholds of the $s$, $p$, and $d$ states to the binding energies of their adiabatic continuations in the high ionizing field. If we define a Stark quantum number $n_s$, then in high field $W = -\frac{1}{2}n_s^{-2}$, and we expect the threshold field for ionization to exhibit an $n_s^{-4}$ dependence. We know that the $s$, $p$, and $d$ states pass adiabatically from low to high field so that we can estimate their paths and hence their energies in high fields by applying the no-crossing rule to states of the same $|m_l|$. The result of this is shown in Fig. 12. For example, the adiabatic continuations of the $17p$, $18s$, and $17d$ states, which we shall still call $17p$, $18s$, and $17d$ for convenience, all go to high-field states which have an energy roughly midway between the $16d$ and $17d$ states in zero field. Since the zero-field $d$ states have essentially zero quantum defects, the high-field quantum numbers of these states are $\sim 16\frac{1}{2}$. From Fig. 12 it is apparent that for an $s$ state $n_s \cong n - \frac{3}{2}$ and for $p$ and $d$ states $n_s \cong n - \frac{1}{2}$.

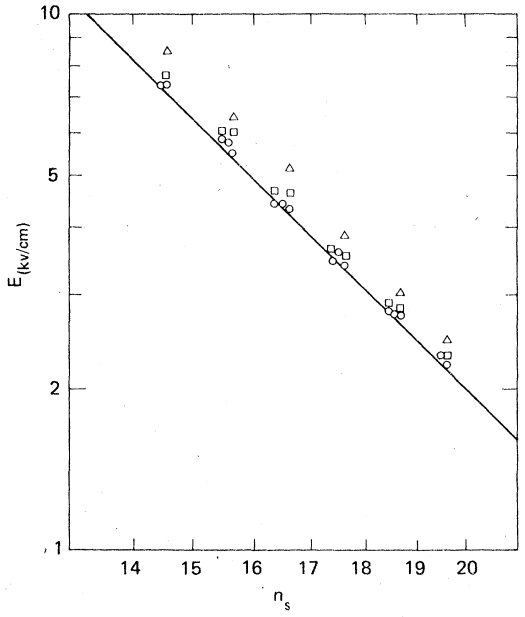


FIG. 13. A plot of threshold field vs $n_s$ (the effective quantum number for the state in a high field) for $|m_l| = 0$ (○), $|m_l| = 1$ (□), and $|m_l| = 2$ (Δ) states. The line indicates the classical ionization threshold.

In Fig. 13 we have plotted on a logarithmic scale the $|m_l| = 0$, 1, and 2 ionization thresholds for the $s$, $p$, and $d$ states vs $n_s$ (the $s$, $p$, and $d$ data may be discerned in Fig. 13 by noting that in order of increasing $n_s$ they are $p$, $s$, and $d$). In Fig. 13 the data for each value of $|m_l|$ lies along a line regardless of whether they are from $s$, $p$, or $d$ states. Had we used either the actual principal quantum number $n$ or the effective low-field quantum number $n^*$ the data from $s$, $p$, and $d$ states would not lie on a line. Thus we feel that relating the ionization thresholds to $n_s$ is indeed a useful way of approaching the problem.

In addition to the data we have also plotted the classical field for ionization of $|m_l| = 0$ states $E = 3.21 \times 10^8 n_s^{-4}$ V/cm which is very close to our observed $|m_l| = 0$ points. Fitting the points of Fig. 13 to an $n_s^{-4}$ dependence yields the following threshold field behavior for $|m_l| = 0$, 1, and 2.

$$\begin{aligned} |m_l| &= 0, \quad E = 3.2(1) \times 10^8 n_s^{-4} \text{ V/cm}, \\ |m_l| &= 1, \quad E = 3.3(1) \times 10^8 n_s^{-4} \text{ V/cm}, \\ |m_l| &= 2, \quad E = 3.8(2) \times 10^8 n_s^{-4} \text{ V/cm}, \end{aligned} \tag{1}$$

The observation that it is progressively more difficult to ionize $|m_l| = 0$, 1, and 2 states of the same energy may be understood at least qualitatively in a fairly simple way. Assume that the electric field is in the $-z$ direction so that upon field ionization the electrons escape from the atom in the $z$ direction. Consider first an atom in an $|m_l| = 0$ state, in which case the valence electron has no kinetic energy invested in its angular momentum. On the other hand, the higher $|m_l|$ states have progressively more energy invested in their angular momenta along the $z$ axis. This energy is the kinetic energy of the electron's motion perpendicular to $z$, which is not useful in penetrating the potential barrier for ionization. Thus, if we have two states of the same energy but different $|m_l|$, the state of higher $|m_l|$ has less energy useful in field ionizing the atom. Consequently, we would expect that $|m_l| = 0$, 1, and 2 states would have progressively higher ionization thresholds, which is what we have observed. This suggests that if the measurements were extended to $|m_l| > 2$ we would find that the higher $|m_l|$ would show progressively higher ionization thresholds.

## VI. CONCLUSION

The ionization threshold and adiabatic passage experiments described here provide a fairly complete picture of the field ionization process enabling us to treat all the Na field ionization data in a general fashion. Na is a fairly typical atom in that it has states for which the manifolds are strongly coupled ($|m_l| = 0$ and 1) as well as states for which the manifolds are weakly coupled ($|m_l| \geq 2$). This suggests that the analysis of the previous section could be applied equally well to many Rydberg atoms. Thus we expect that the field ionization behavior of many atoms could be predicted by simply estimating the location of the adiabatic high-field levels as shown in Fig. 12 and using the $|m_l|$ dependence of the threshold fields shown in Eq. (1). These experiments suggest that a classical approach is useful in understanding the problem, and we hope these experiments will stimulate theoretical interest in the problem of field ionization of coupled Stark manifolds.

Aside from its fundamental interest, a good understanding of the field ionization process is important because field ionization will undoubtedly be used in many experimental applications because the method is simple, highly selective, and ~100% efficient. The method has already been used to observe radio frequency transitions and to analyze collision products. Application to such diverse problems as far-infrared, microwave photon detection, and laser isotope separation have been suggested.

## ACKNOWLEDGMENT

We are grateful to D. C. Lorents for critical readings of the manuscript.

---

*This work supported in part by the Electric Power Research Institute and in part by Stanford Research Institute.

[1]H. A. Bethe and E. A. Salpeter, *Quantum Mechanics of One and Two Electron Atoms* (Academic, New York, 1957).

[2]M. H. Rice and R. H. Good, Jr., J. Opt. Soc. Am. 52, 239 (1962).

[3]D. S. Bailey, J. R. Hiskes, and A. C. Riviere, Nucl. Fusion 5, 41 (1965).

[4]D. R. Herrick, J. Chem. Phys. 65, 3529 (1976).

[5]R. N. Il'in, *Atomic Physics*, Vol. 3, edited by S. J. Smith and G. K. Walters (Plenum, New York, 1973).

[6]J. E. Bayfield and P. M. Koch, Phys. Rev. Lett. 33, 258 (1974).

[7]T. W. Ducas, M. G. Littman, R. R. Freeman, and D. Kleppner, Phys. Rev. Lett. 35, 366 (1975).

[8]A. F. J. van Raan, G. Baum, and W. Raith, J. Phys. B 9, L173 (1976).

[9]R. F. Stebbings, C. J. Latimer, W. P. West, F. B. Dunning, and T. B. Cook, Phys. Rev. A 12, 1453 (1975).

[10]D. H. Tuan, S. Liberman, and J. Pinard, Opt. Commun. 18, 533 (1976).

[11]M. G. Littman, M. L. Zimmerman, and D. Kleppner, Phys. Rev. Lett. 37, 486 (1976).

[12]T. F. Gallagher, L. M. Humphrey, R. M. Hill, and S. A. Edelstein, Phys. Rev. Lett. 37, 1465 (1976).

[13]T. F. Gallagher, L. M. Humphrey, R. M. Hill, W. E. Cooke, and S. A. Edelstein (unpublished).

[14]T. W. Hänsch, Appl. Opt. 11, 895 (1972).

[15]V. W. Hughes and L. Grabner, Phys. Rev. 79, 829 (1950).